



Original scientific paper

A preliminary study into the effect of oxide chemistry on the bonding mechanism of cold-sprayed titanium dioxide coatings on SUS316 stainless steel substrate

Noor Irinah Binti Omar^{1,✉}, Suhana Binti Mohamed², Yusliza Binti Yusuf¹, Toibah Binti Abdul Rahim³, Zaleha binti Mustafa³, Syahriza Binti Ismail³, Ilyani Akmar Binti Abu Bakar⁴ and Santirraprahkash Selvamani⁵

¹Faculty of Mechanical and Manufacturing Engineering Technology, Universiti Teknikal Malaysia Melaka, Hang Tuah Jaya, 76100 Durian Tunggal, Melaka, Malaysia

²Faculty of Business management, Universiti Teknologi Mara Johor, kampus pasir gudang, Jalan purnama, Bandar seri alam, 81750, Masai, Malaysia

³Faculty of Manufacturing Engineering, Universiti Teknikal Malaysia Melaka, Hang Tuah Jaya, 76100 Durian Tunggal, Melaka, Malaysia

⁴School of Civil Engineering, College of Engineering, Universiti Teknologi Mara, 40450, Shah Alam, Selangor, Malaysia

⁵Department of Mechanical Engineering, Toyohashi University of Technology, 1-1 Tempaku-Cho, Toyohashi, Aichi 441-8580, Japan

Corresponding author: ✉ nooririnah@utem.edu.my; Tel.: +60123661044; Fax: 606-2701064

Received: June 22, 2022; Accepted: July 25, 2022; Published: August 10, 2022

Abstract

Current attention has focused on the preparation of thick ceramic coating of nano-structured materials as feedstock material using the thermal spray process. The cold spray method has appeared as a promising process to form ceramic nanostructured coating without significantly changing the microstructure of the initial feedstock materials due to its low processing temperature. However, deposition of ceramic powders by cold spray is not easy due to the brittle characteristics of the material. In this study, TiO₂ coatings were deposited on unannealed stainless steel substrates and substrates that were annealed from room temperature to 700 °C prior to spraying. The adhesion strength was evaluated to investigate the bonding mechanism. The influence of the remaining surface oxide layer of chromium oxide, Cr₂O₃, which is thermodynamically preferred for stainless steel, on the bonding mechanism involved was investigated. The results showed that by increasing the annealing substrate temperature of stainless steel, the adhesion strength of the coatings (thicker oxide) is also increased. As a result, the bonding between the cold-sprayed TiO₂ particle and the steel substrate is given by the chemical bonding of an inter-oxide reaction.

Keywords

TiO₂ coatings, chromium oxide, adhesion strength, bonding mechanism.

Introduction

Cold spraying is a solid state process in which powder feedstock in the range of 5 to 40 nm in the powder feeder is supersonically accelerated in the De-Laval part of the nozzle and then passed through the nozzle to form a coating on a substrate [1]. When the particle velocity exceeds the critical velocity, the plastic deformation of both, the sprayed metallic particle and the metallic substrate, removes the surface oxide layers, exposing newly formed surfaces. The metallic bond is formed on the newly formed surface, and cold spray deposition may follow. For formation jetting, the contact between the particles and the substrate is extruded. Material flow at the interface is defined as shear instability for bonding formation [2-4]. This solid powder deposition approach can reduce oxidation and other negative impacts on coating characteristics induced by the high-temperature procedure [5-7].

It is well known that cold spraying of ceramic materials can be difficult because cold spraying requires plastic deformation of the feedstock particles for adhesion to the substrate. The difficulty lies in making hard and brittle ceramic materials such as TiO₂ deform plastically. However, previous studies reported the possibility of cold spraying thick pure TiO₂, but the bonding mechanism of cold sprayed TiO₂ is not fully understood yet [8].

Few researchers have proposed chemical bonding as a bonding mechanism in the cold spray process, especially in the cases of ceramic cold spray like TiO₂, where a TiO₂ coating was produced from recombination of broken up crystallite links during the cold spray process, which was initiated by the porous structure of the agglomerated powders [9]. They proposed that chemical bonding may allow thick coatings to be deposited by the cold spray process. The agglomerated powder in nano-scale primary particles containing nano porosity was fractured, leaving an unstable surface with a dangling bond structure. To reobtain a stable surface, the fractured particles decoupled and formed a surface with improved stability, which led to the bonding of the newly impacting particles and building up the coating [9]. Salim *et al.* [10] prepared 400 μm and 150 μm thick TiO₂ coatings on metal and tile, respectively. It was observed that adhesion strength changed little with spraying parameters. This indicated that mechanical interlocking was not the main bonding mechanism in this case, so was the substrate shear instability. It was discovered that both the hardness and the oxidizability of the substrates affected the adhesion strength of TiO₂ coatings. The adhesion strength of TiO₂ coatings could be improved by changing the surface chemistry of the substrates. It was proposed that the chemical or physical bonding mechanism was the main bonding mechanism of ceramic coating. TEM images proved the existence of chemical bonding between TiO₂ particles. Preheating could increase the oxidizability of the substrate, thus deteriorating the adhesion strength of coatings. Gardon *et al.* [11] reported that the mechanism responsible for the deposition of TiO₂ on the stainless-steel substrate in the cold-spraying process is the chemical bonding between particles and substrate. They have shown that the previous layer of titanium sub-oxide prepares the substrate with the appropriate surface roughness needed for the deposition of TiO₂ particles on the substrate surface.

From the previous results and discussion above, it is clear that cold spray coating of TiO₂ is not easy to be obtained, but not impossible. Also, there is still considerable uncertainty concerning the bonding mechanism involved for pure TiO₂ powder metal substrates, especially focusing on the mechanism of chemical bonding. This paper is a preliminary study to study the effect of oxide chemistry on the bonding mechanism of cold sprayed titanium dioxide coating on stainless steel, SUS316.

Experimental

Materials

We employed agglomerated TiO₂ powder (WP0097, TAYCA Corporation, Tokyo, Japan) as a feedstock with a pure anatase crystalline structure and an average particle size of around 7.55 nm, as shown in Figure 1. The substrate is stainless steel, SUS316.

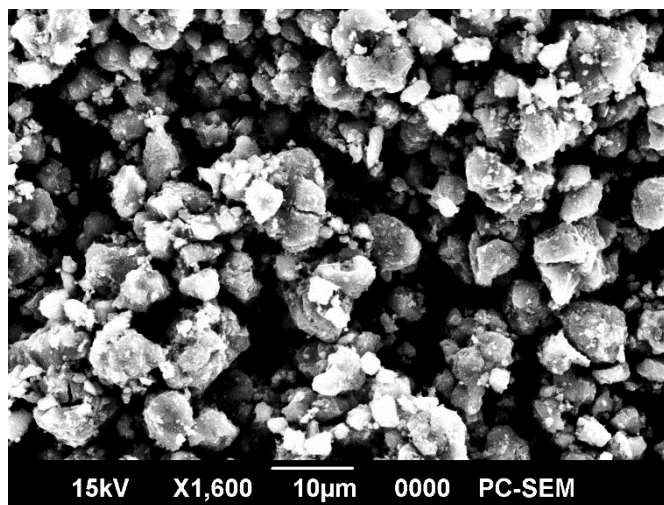


Figure 1. SEM image of TiO₂ powder

Cold spray process

All the coating attempts were carried out with cold spraying equipment and a De-Laval 24TC nozzle (CGT KINETIKS 4000; Cold Gas Technology, Ampfing, Germany). At 500 °C working temperature, nitrogen was employed as the process gas. The pressures of 3 MPa, with a process traverse speed of 10 mm/s and a spray distance of 20 mm were utilized.

Characterizations

Strength testing

Specimen areas of ϕ 25×10 mm were utilised to assess the coatings adhesive strength, which was supplied as the fracture load amount recorded by a universal testing machine, Autograph AGS-J Series 10 kN, Shimadzu, Japan, in compliance with Japan industrial standard H 8402. The adhesion strength of each spraying condition using a means of five specimens was tested. On the fracture coating surface, EDX was used.

Coatings evaluation

The cross-sectional microstructure of the TiO₂ coating on annealed substrates was analyzed *via* a scanning electron microscope (SEM: JSM-6390, JEOL, Tokyo, Japan).

Micro Vickers hardness

The hardness investigation was HV 0.1 with a test force on the cross-section of 98.07 mN at a dwell time of 10 s.

Oxide composition of the substrate and TiO₂ coating interface evaluation by XPS

X-ray photoelectron spectrometer (XPS) was used to investigate the effect of the atomic and chemical composition of the substrate oxide layer on the adhesion strength of agglomerated TiO₂ coating. In addition, the chemical composition of the TiO₂ coating and the substrate interface was

also investigated by XPS to identify if a change in chemical composition was present after coating formation by the cold gas spray method.

Table 1 shows the conditions of the XPS analysis for substrate oxide analysis. Tables 2 and 3 show the XPS analysis conditions for TiO₂ coating and substrate interface analysis. The peak position was corrected with the C1s peak set at 285 eV. When pre-sputtering to clean the surface was performed, the sample surface was reduced and the measurement results were affected, so XPS analysis was performed without pre-sputtering.

Table 1. XPS parameters (substrate oxide layer analysis)

Measured regions	Fe 2p, O 1s, Cr 2p, Mn 3d
Measured X-ray output energy, W	10
Probe diameter, μm	50
Time per step, ms	30
Pass energy, eV	140
Number of cycle	30

Table 2. XPS parameters (TiO₂ / substrate interface wide scan)

Measured regions, eV	0-1100
Measured X-ray output energy, W	10
Probe diameter, μm	50
Time per step, ms	5.2
Pass energy, eV	140
Number of cycle	5

Table 3. XPS parameters (TiO₂ / substrate interface narrow scan)

Measured regions	Fe 2p, Cr 2p
Measured X-ray output energy, W	10
Probe diameter, μm	50
Time per step, ms	5.2
Pass energy, eV	55
Number of cycle	5

Results and discussion

Coating adhesion strength

Figure 2 shows the coating tensile strength of TiO₂ on left x-axis and Vickers hardness on right x-axis for annealed stainless steel, SUS 316 from room temperature to 700 °C annealed. The result shows an increasing trend in the coating adhesion strength from 1.00 MPa to 1.88 MPa as the annealed substrate temperature increases from room temperature to 700 °C, but substrate hardness shows an opposite trend. Figure 3 shows the image of the fractured surface of the substrate and TiO₂ coating after the tensile strength test was conducted. This image confirms that the fracture was an interfacial fracture of substrate and coating, proving thus that a strong, cohesive bond among TiO₂ particles has been achieved during the coating formation process. It was observed that adhesion strength changed little with the change of spraying parameters. This indicated that mechanical interlocking was not the main bonding mechanism, in this case, so was the substrates

shear instability. It was discovered that both the hardness and the oxidizability of the substrates affected the adhesion strength of TiO₂ coatings. The adhesion strength of TiO₂ coatings could be improved by changing the surface chemistry of the substrates. It was proposed that the chemical or physical bonding mechanism was the main bonding mechanism of ceramic coating. In order to confirm the surface chemistry factor, substrate analysis will be discussed further in this paper.

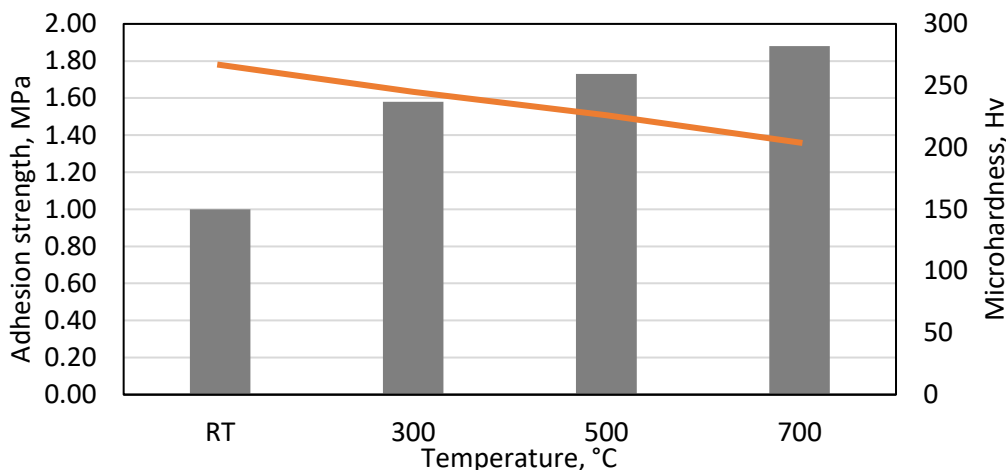


Figure 2. Adhesion strength (■) of the titanium dioxide coating on annealed SUS316 and substrate hardness (—) for different annealed substrate temperature



Figure 3. Fractured surface of substrate and TiO₂ coating after tensile strength test

Cross-sectional observation of substrate and TiO₂ coating

The cross-sectional microstructure of substrate and TiO₂ coating observed under SEM is shown in Figures 4 (a) and (b).

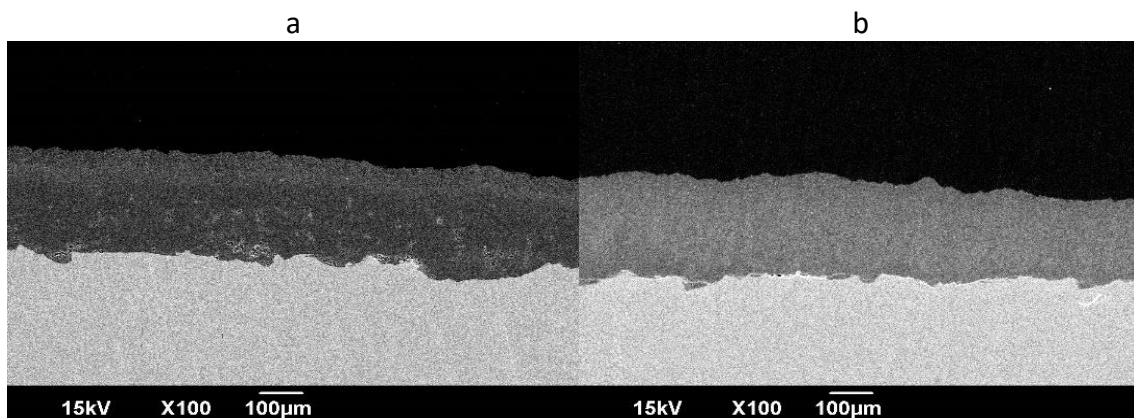


Figure 4. Cross-sectional microstructure of SUS316 and TiO₂ coating: (a) room temperature (b) 700 °C annealed

Substrates treated at room temperature and 700 °C were chosen for observation to clarify the interface adhesion between substrates which yielded the lowest and highest adhesion strength. Coating with a thickness in the range of 200 to 300 µm was measured, showing that the critical

velocity of particles was reached during the spraying process. Meanwhile, the interface area of both types of substrates treated at room temperature and 700 °C shows good adhesion with visibly fewer cracks. This shows that the 700 °C annealing process minimizes the interface adhesion between the substrate and TiO₂ coating.

Depth profile analysis of oxide layer

The depth analysis of the oxide layer by X-ray photoelectron spectroscopy for SUS 316 substrate is shown in Figures 5 (a) to (d) for the samples treated from room temperature to 700 °C. SiO₂ equivalent depth refers to the sputter etching rate to measure depth profiling measurement in this experiment. The sputter etching rate is generally estimated from an elemental depth profile of a standard sample with a known thickness, such as a SiO₂ film.

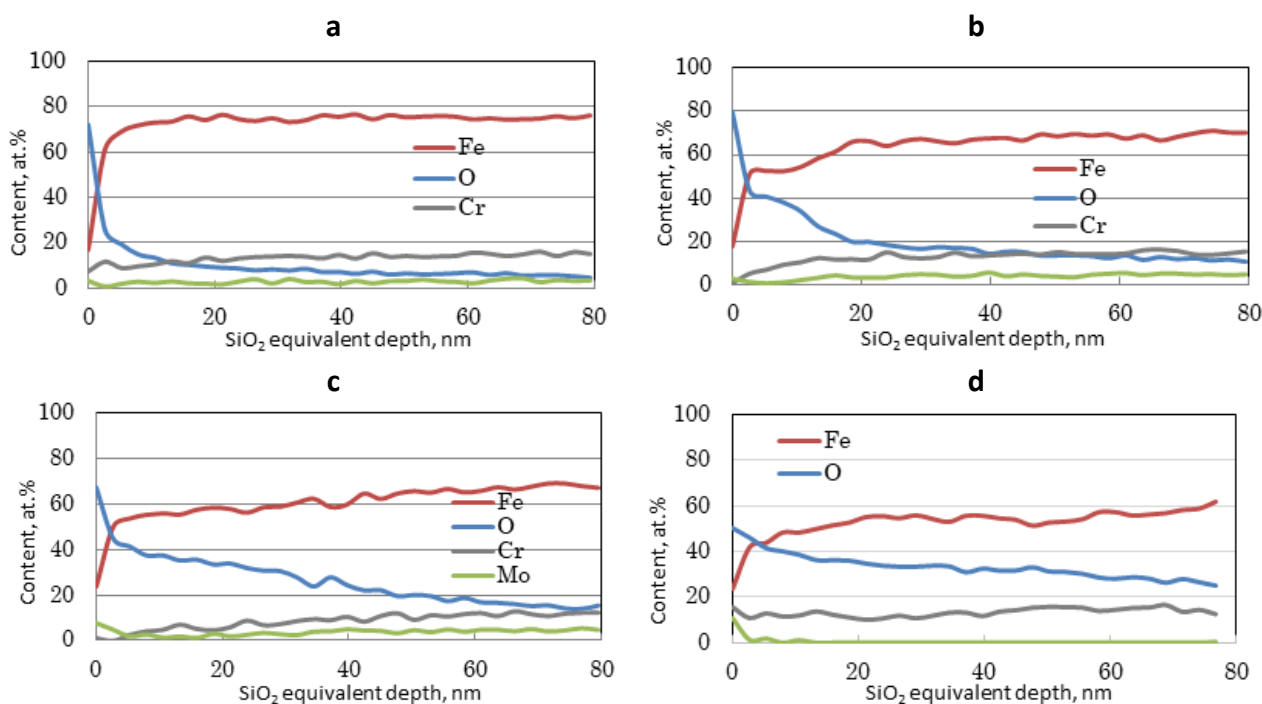


Figure 5. Depth profile analysis of stainless steel, SUS316: (a) room temperature (b) 300 °C annealed (c) 500 °C annealed and (d) 700 °C annealed

This shows that the stainless steel oxide layer thickens as the substrate annealing temperature rises. The surface of the substrate plays an important role in achieving high adhesion strength of the cold sprayed coatings. This is because the adhesive strength of the coating is specifically determined by the bonding of the first layer of TiO₂ particles with the outermost surface of the substrate. When metal is used as a substrate, the outermost surface will always be composed of a passive oxide layer with a few nanometers of thickness. Since the agglomerated TiO₂ particles will break down during contact with the surface of the substrate [9], it can be assumed that the first layer of contact between particles and substrate will be achieved in an area that is a few nanometers deep from the top surface of the oxide layer.

The atomic composition of iron on the outermost surface of the oxide layer increases slightly as the annealing temperature increases. However, since the increment is small, it can be considered that this slight change has not affected the increase of the adhesion strength. The atomic composition of oxygen in the deepest part of the oxide layer increases significantly as the annealing temperature increases. This shows that the oxide layer of stainless steel grows thicker as the annealing temperature of the substrate increases. The increase in oxide thickness might have played

a role in the increasing trend of adhesion strength because the substrate oxide layer and feedstock powder, TiO_2 , are made of oxide material. The behaviour of the chromium oxide is seen to have changed the most as the annealing temperature increases. In SUS 316, the atomic composition of chromium at the outermost surface of the oxide layer decreases to near depletion as the annealing temperature increases from room temperature to 500 °C. This phenomenon has been reported in other research [12] known as chromium depletion. However, as the annealing temperature is raised to 700 °C, the amount of chromium at the outermost surface for SUS 316 increases significantly. This sudden change can be considered a factor affecting the increases in adhesion strength.

Evaluation of the chemical state of iron and chromium in the oxide layer by X-ray photoelectron spectroscopy

Figure 6 (a) shows the peak position of iron, approximately at 706.7 eV. It was prominently present in the oxide layer for the room temperature substrate. This concludes that the oxide layer was thin for the not annealed substrate. At annealing temperatures of 300 and 500 °C, the peak position of magnetite Fe_3O_4 (Fe^{2+}) at approximately 709.3 eV was detected at the outermost surface of the SUS 316 substrate. Below 570 °C, the wüstite state of iron oxide (Fe_{1-x}O , $x = 0.84-0.95$) is unstable, and the oxidation of iron directly results in magnetite or ferrite [8]. At the highest annealing temperature of 700 °C, the oxide layer consists of a two-layered microstructure with a thin outer layer of hematite Fe_2O_3 and a secondary layer of magnetite Fe_3O_4 (Fe^{2+}) at 710.7 eV [13].

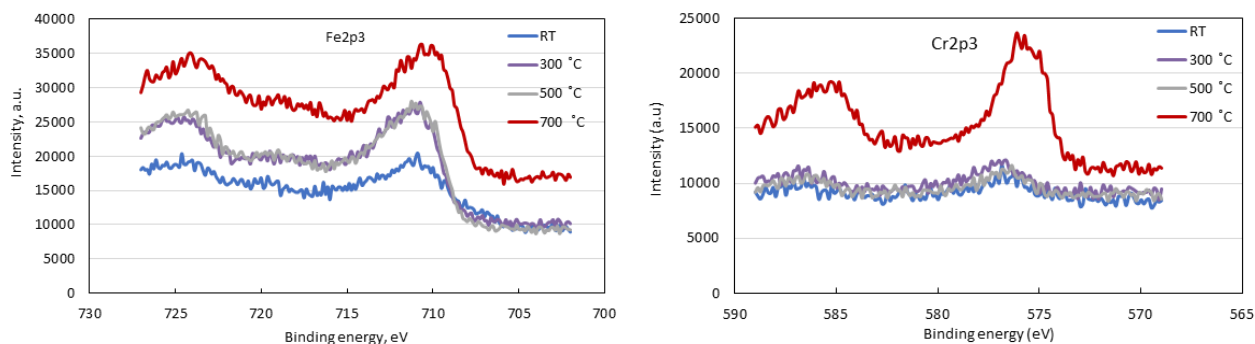


Figure 6. XPS spectra of (a) iron and (b) chromium for annealed SUS316

Figure 6 (b) shows the peak of chromium at 574 eV, which was prominently present in the oxide layer for the room temperature substrates of SUS 316. The peak position of chromium oxide at 576 eV was absent at the outermost layer of the oxide for both substrates at annealing temperatures of 300 and 500 °C. This shows that the chromium depletion phenomenon occurred at these temperatures [12]. However, at an annealing temperature of 700 °C, the peak position of chromium oxide, Cr_2O_3 , is present throughout the outermost and intermediate surface of the oxide layer for SUS 316 substrates. This indicates that one of the major components of the oxide layer at 700 °C is chromium oxide, Cr_2O_3 .

Evaluation of oxide composition at the interface of coating by X-ray photoelectron spectroscopy

Figure 7 shows the schematic image of the evaluation of oxide composition at the interface by XPS. The wide scan analysis of the coating interface indicates the presence of peak positions for titanium, oxygen, carbon and sodium. The traces of iron and chromium were not detected through the wide scan analysis, as shown in Figure 8 (a). The narrow scan analysis shows that iron elemental peak was absent at the coating interface, but the chromium elemental peak was detected at trace amounts.

The peak position (577 eV) indicates that chromium oxohydroxyde, CrOOH, was present, as shown in Figures 8(b) and 8(c).

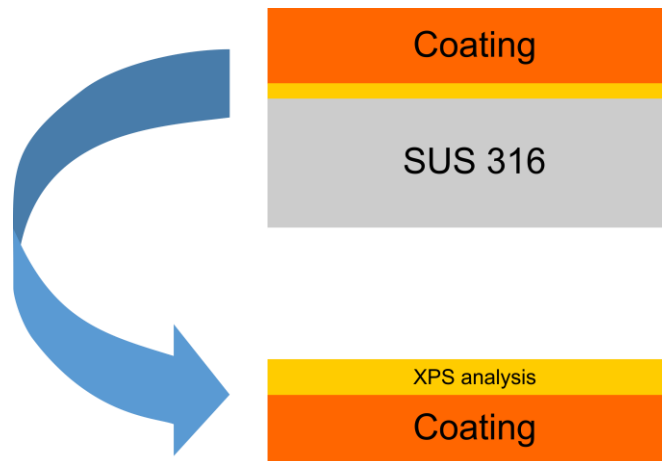


Figure 7. Schematic image of evaluation of oxide composition at the interface

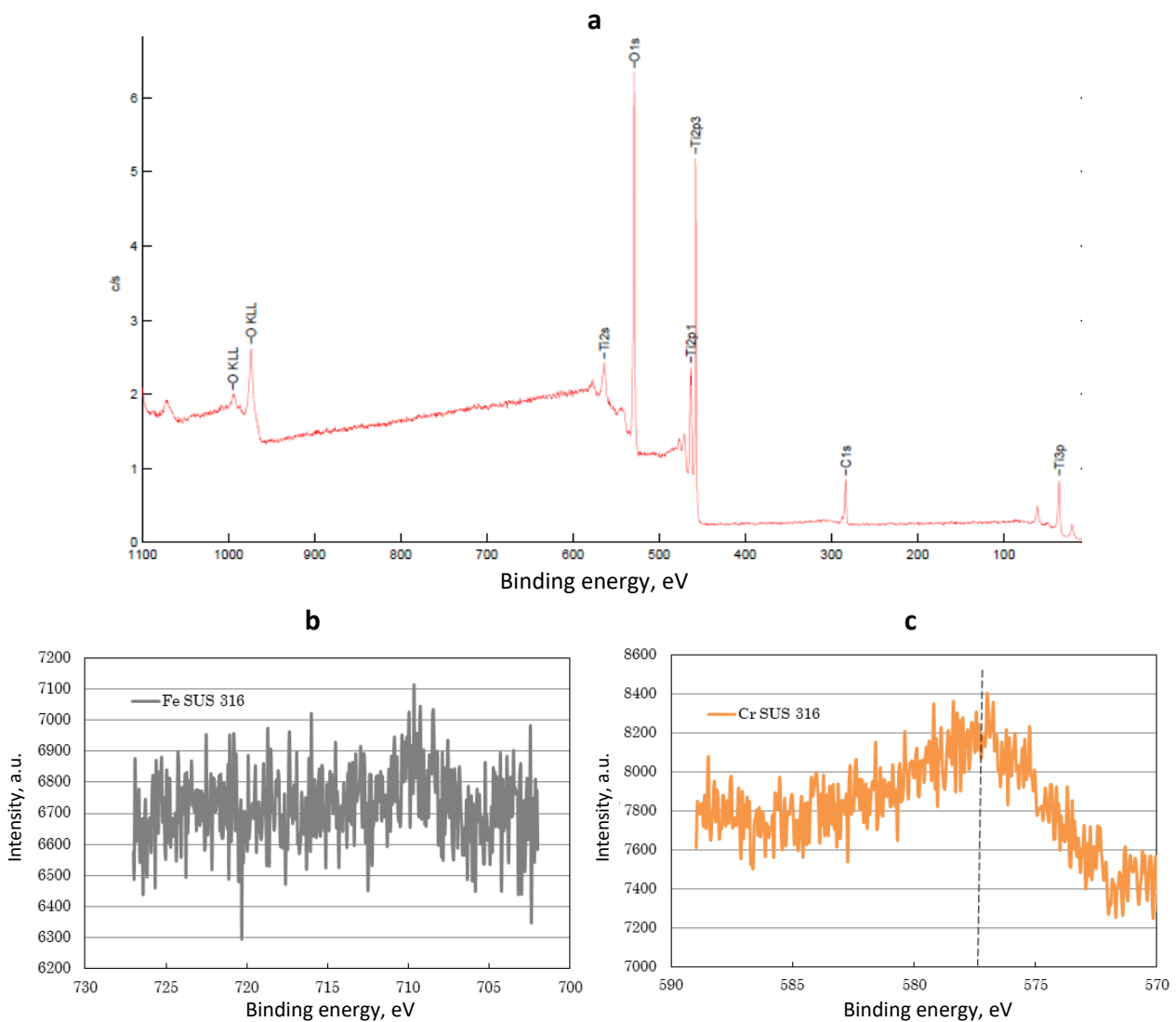


Figure 8. XPS spectra (a) wide scan, (b) narrow scan for iron and (c) narrow scan for chromium

The chemical state of chromium changed from Cr₂O₃ to CrOOH after the cold spray coating process. It can be assumed that this change in chemical state has affected the increase in adhesion strength.

However, the trace amount of chromium oxohydroxyde detected might have been the product of the reaction between chromium oxide, Cr_2O_3 , present at the outermost surface of the oxide layer and water molecules present in the atmosphere during the cold spray process.

The thickness of the oxide layer on the substrate surface increased as the temperature of the substrate increased during annealing. Oxide analysis was performed to confirm this situation. The atomic concentration of oxygen in the oxide film was raised significantly as the temperature of the annealing material rose from room temperature to 700 °C. This indicates that as the annealing temperature rises, the oxide layer of SUS316 substrate becomes thicker.

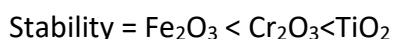
The literature indicates that bonding in the cold spray is governed by mechanical interlocking and metallurgical bonding. Severe plastic deformation at the interface, owing to the high energy impacts of the particles, breaks the native oxide layers of the interacting surfaces. The disruption of oxide layers facilitates the penetration of particles into the substrate, which leads to the jet formation and mechanical interlocking [14]. Ichikawa *et al.* [15] investigated the effect of substrate conditions on the deposition process, finding out that the initial oxide film thickness has a substantial effect on the deposition efficiency. Yin *et al.* [16] claimed that in addition to the substrate hardness, the particle velocity and the spray angle can influence the deformation behaviour and final state of the oxide film. Moreover, the results indicate that the formation of a fresh metal surface followed by immediate contact with the mating material, which can be a metal or oxide, is a necessary condition to form intimate bonding in a kinetic spraying process. Many researchers have observed adhesion between metal coatings and smooth ceramic substrates. This suggests that mechanical interlocking is not necessary for adhesion and a physico-chemical interaction at the metal/ceramic interface significantly contributes to adhesion [17-19].

Our findings revealed that as the oxide thickness on the SUS316 substrate increased due to the annealing process, the coating adhesion strength increased steadily. This trend seems reversed from the mechanical or metallurgical bonding mechanism, which requires an oxide-free surface to form intimate contact between particle/substrate and provide good adhesion bonding. Chemical oxide analysis was conducted to further understand how oxide thickness plays a role in the bonding mechanism.

The chemical composition of the oxide layer for hard metals substrate is depicted earlier in this paper and the annealed 700 °C SUS316 oxide consists of a mixture of Fe_2O_3 and Cr_2O_3 in the outermost layer.

The Ellingham-Richardson diagram [20], as shown in Figure 9 below, is utilized to show the standard free energy of formation for oxides as a function of temperature and equilibrium oxygen partial pressure at 200 °C as indicated by the red-dotted line and blue arrow for iron, chromium, and titanium. The gas temperature was 500 °C and referring to previous work in our lab, 200 °C was the temperature on the substrate when the coating was formed. Gibbs equation helps us predict reactions' spontaneity directly based on enthalpy and entropy values. Thus, when the reaction is exothermic, the enthalpy of the system is negative, making Gibbs free energy negative. Hence, we can say that the reaction will proceed in the forward direction due to a positive value of the equilibrium constant. This law can also be scaled for two different reactions in a system. The overall reaction (combination of two reactions) will occur only if the net ΔG (sum of ΔG s of both reactions) of the two possible reactions is negative [21].

Based on Figure 9, we can arrange metal oxide for substrates involved as follows:



The oxidation process of metal generally depends on its thermodynamics and kinetics. The relationship between the standard Gibbs free energy change, ΔG° , and temperature T [22] is presented by equations (1) and (2):

$$\Delta G^\circ(\text{Fe}_2\text{O}_3) = -543.349 \text{ J/mol} + 167.4 \text{ (J/mol K)}T \tag{1}$$

$$\Delta G^\circ(\text{Cr}_2\text{O}_3) = -746.844 \text{ J/mol} + 173.2 \text{ (J/mol K)}T \tag{2}$$

ΔG° will be less than 0 when T changes within a certain range, indicating that the reaction favors the generation of oxides. Moreover, ΔG° for Cr_2O_3 is always more negative than ΔG° (Fe_2O_3) at the same T , implying the greater affinity of oxygen to chromium. Therefore, the Cr_2O_3 formation is thermodynamically preferred on the SUS316 substrate. Meanwhile, for the Fe atom, although the thermodynamics of its oxidation process is not dominant, it is the most mobile atom in the oxide film [16]. Therefore, the Fe_2O_3 formation is controlled more by kinetics than thermodynamics.

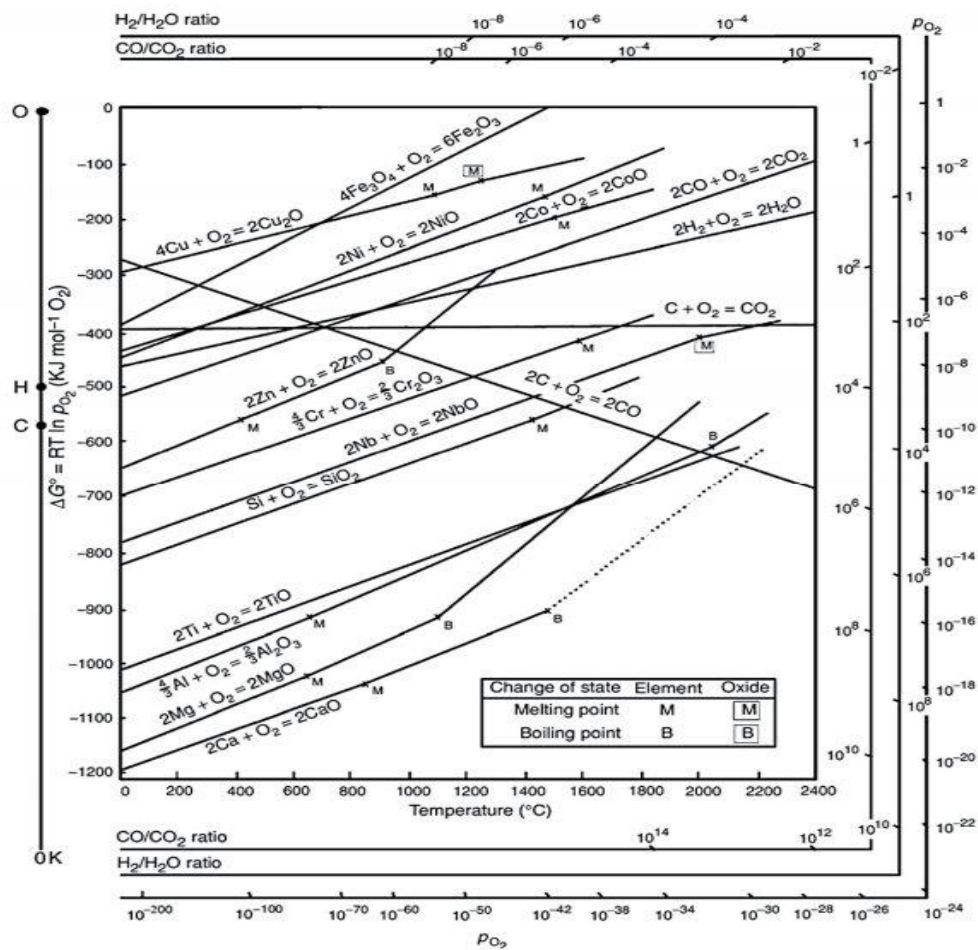


Figure 9. Ellingham-Richardson diagram for selected elements [20]. Reproduced with permission from ref. [20], Copyright (2018), University of Cambridge

The mechanisms of cold spraying of metal particles on ceramics or glass involve more factors, such as the chemical properties of impact particles and substrates. Song *et al.* [18] used cold spraying of Al particles on a glass substrate. The interlayer with a thickness of 80 nm between impacted Al particles and glass substrate was composed of an amorphous phase and nanocrystalline grains with significant Na enrichment. The layer is considered to form as a result of the reaction between the impacted Al and the glass substrate, which took place due to the temporal high temperatures during impact, which produced liquid phases at the interface. It is believed that the high affinity of Al with oxygen in the glass substrate enabled the relatively strong adhesion

observed. Our coating adhesion strength on hard metals substrate is in good agreement with the report of Song *et al.* [18].

TiO₂ has a characteristic structure of bridging oxygen atom rows along the [001] direction, six-fold-coordinated (6c or 6f) Ti atoms below the bridging oxygen and five-fold-coordinated (5c or 5f) Ti atoms in troughs between bridging oxygen rows, as shown in Figure 10. The bridging oxygen vacancy (O_{br}) is a common defect on TiO₂. Such oxygen vacancies can be created by annealing the surface at a high temperature or bombarding with electrons [23]. For each O_{br}, two excess electrons remain on the surface. Consequently, TiO₂ becomes rather reactive to the dissociation of electrophilic adsorbates such as O₂ and H₂O. Hence, it is important to understand the electronic structure of the defective TiO₂ surfaces.

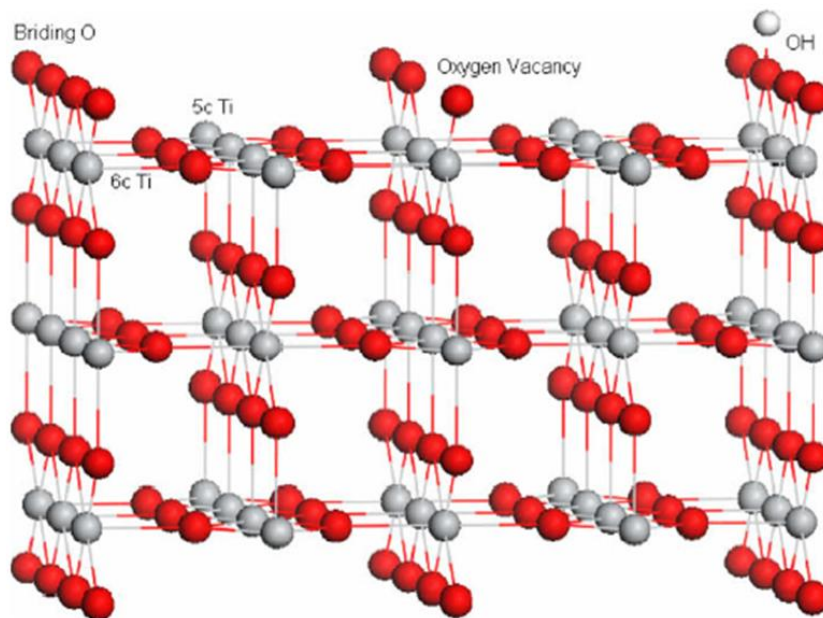


Figure 10. Side view of the TiO₂ surface with one oxygen vacancy and OH group. O atoms are represented by red spheres and Ti atoms by grey spheres. *Reproduced with permission from ref. [23], Copyright (2009), Elsevier*

Kim *et al.* [17] used kinetic spraying of single titanium particles on mirrored steel substrates. They showed that some portion of a thin amorphous oxide remained between the particle-substrate interface and even a severe plastic deformation was associated with the impacts of the particles onto the substrate. The remaining oxide provided a bond between a particle or particle-substrate. It was observed that adhesion strength changed little with spraying parameters. This indicated that mechanical interlocking was not the main bonding mechanism, in this case, so was the substrates' shear instability. It was discovered that both the hardness and the oxidizability of the substrates affected the adhesion strength of TiO₂ coatings. The adhesion strength of TiO₂ coatings could be improved by changing the surface chemistry of the substrates. It was proposed that the chemical or physical bonding mechanism was the main bonding mechanism of ceramic coating. TEM images proved the existence of chemical bonding between TiO₂ particles. By the way, preheating could increase the oxidizability of the substrate, thus deteriorating the adhesion strength of coatings. The result seems to be in agreement with the chemical bonding mechanism.

Yamada *et al.* [9] reported that the agglomerated powder of TiO₂ in nano-scale primary particles, which also contained nanoporosity, was fractured, leaving an unstable surface with a dangling bond structure. The fractured particles decoupled and formed a surface with improved stability to reobtain

a stable surface, which led to the bonding of newly impacting particles and coating building [4]. When high-velocity cold sprayed TiO₂ particle impacted on annealed stainless steel that already consists of oxide mixture Cr₂O₃+Fe₂O₃ on the top surface, inter oxide reaction occurs. TiO₂ particles that already have oxygen vacancy will break at collision and bond again to give cohesion and adhesion bonding by inter oxide reaction TiO₂-Cr₂O₃ from chromium oxide on SUS316 that is thermodynamically preferred compared to Fe₂O₃.

Conclusions

Coating adhesion strength on stainless steel showed an increasing trend as the substrate annealing temperature increased (thicker oxide). The primary bonding mechanism of TiO₂ particle and SUS316 substrate is chemical bonding by inter-oxide bonding, which is provided by a chemical reaction of TiO₂-OH⁻, where OH⁻ is provided by chromium oxide, Cr₂O₃, which is thermodynamically preferred on SUS316. However, further precise research with the usage of pure chromium substrates is needed to clarify the change in the chemical states of elements after the cold spray process.

Acknowledgements: We acknowledge the Interface & Surface Fabrication Lab, Toyohashi University of Technology, Majlis Amanah Rakyat, MARA and Universiti Teknikal Malaysia Melaka, UTeM for Noor Irinah's scholarship.

References

- [1] A. Papyrin, V. Kosarev, S. Klinkov, A. Alkhimov, V. M. Fomin, *Cold Spray Technology*, Elsevier, Amsterdam, The Netherlands, 2006, p. 70-96. ISBN: 9780080465487. <https://www.elsevier.com/books/cold-spray-technology/papyrin/978-0-08-045155-8>
- [2] H. Assadi, F. Gärtner, T. Stoltenhoff, H. Kreye, *Acta Materialia* **51(15)** (2003) 4379-4394. [https://doi.org/10.1016/S1359-6454\(03\)00274-X](https://doi.org/10.1016/S1359-6454(03)00274-X)
- [3] T. Schmidt, F. Gärtner, H. Assadi, H. Kreye, *Acta Materialia* **54(3)** (2003) 729-742. <https://doi.org/10.1016/j.actama.2005.10.005>
- [4] T. Schmidt, H. Assadi, F. Gärtner, H. Richter, T. Stoltenhoff, H. Kreye, T. Klassen, *Journal of Thermal Spray Technology* **18** (2009) 794-808. <https://doi.org/10.1007/s11666-009-9357-7>
- [5] F. Gärtner, T. Stoltenhoff, T. Schmidt, H. Kreye, *Journal of Thermal Spray Technology* **15** (2006) 223-231. <https://doi.org/10.1361/105996306X108110>
- [6] T. H. Van Steenkiste, J. R. Smith, R. E. Teets, J. J. Moleski, D. W. Gorkiewicz, R. P. Tison, D. R. Marantz, K. A. Kowalsky, W. L. Riggs II, P. H. Zajchowski, B. Pilsner, R. C. McCune, K. J. Barnett, *Surface Coating Technology* **111(1)** (1999) 62-71. [https://doi.org/10.1016/S0257-8972\(98\)00709-9](https://doi.org/10.1016/S0257-8972(98)00709-9)
- [7] R. Ghelichi, M. Gualiagno, *Journal Frattura ed Integrità Strutturale* **8** (2009) 30-44. <https://doi.org/10.3221/IGF-ESIS.08.03>
- [8] M. Yamada, H. Isago, H. Nakano, M. Fukumoto, *Journal of Thermal Spray Technology* **19** (2010) 1218-1223. <https://doi.org/10.1007/s11666-010-9520-1>
- [9] M. Yamada, H. Isago, K. Shima, H. Nakano, M. Fukumoto, in: *Thermal Spray: Global Solutions to Future Application, Proceedings of the International Thermal Spray Conference, 2010, Singapore*, B. R. Marple, A. Agarwal, M. M. Hyland, Y.-C. Lau, C.-J. Li, R. S. Lima, G. Montavon (Eds.), Springer, 2011, p. 172-176. ISBN-13: 978-1493951901
- [10] N. T. Salim, M. Yamada, H. Nakano, K. Shima, H. Isago, M. Fukumoto, *Surface and Coating Technology* **206(2-3)** (2011) 366-371. <https://doi.org/10.1016/j.surfcoat.2011.07.030>
- [11] M. Gardon, C. Fernández-Rodríguez, D. Garzón Sousa, J. M. Doña-Rodríguez, S. Dosta, G. Cano, J. M. Guilemany, *Journal of Thermal Spray Technology* **23** (2014) 1135-1140. <https://doi.org/10.1007/s11666-014-0087-0>

- [12] K. Nomura, Y. Ujihira, *Journal of Materials Science* **25** (1990) 1745-1750.
<https://doi.org/10.1007/BF01045379>
- [13] X.Yu, J. Zhou, IntechOpen, Chapter 4, 2017, 61-73. <https://doi.org/10.5772/66211>
Y. Ichikawa, R. Tokoro, K. Ogawa, *Proceedings of the International Thermal Spray Conference, ITSC 2018*, pp. 238–241. ISBN 9781627081603.
- [14] Y. Ichikawa, K. Ogawa, *Journal of Thermal Spray Technology* **24** (2015) 1269-1276.
<https://doi.org/10.1007/s11666-015-0299-y>
- [15] S.Yin, X.Wang, W.Li, *Applied Surface Science* **259** (2012) 294-300.
<https://doi.org/10.1016/j.apsusc.2012.07.036>
- [16] K.H.Kim, S. Kuroda, *Scripta Materialia* **63(2)** (2010) 215-218.
<https://doi.org/10.1016/j.scriptamat.2010.03.061>
- [17] M. Song, H. Araki, S. Kuroda, K. Sakaki, *Journal of Physics D* **46** (2013) 195301.
<https://doi.org/10.1088/0022-3727/46/19/195301>
- [18] M. V. Vidaller, A. List, F. Gaertner, T. Klassen, *Journal of Thermal Spray Technology* **24** (2015) 644-658. <https://doi.org/10.1007/s11666-014-0200-4>
- [19] University of Cambridge. The Ellingham diagram in removal of contaminants. Dissemination of IT for the Promotion of Materials Science (DoITPoMS), TLP Library.
<https://www.doitpoms.ac.uk/tlplib/recycling-metals/ellingham.php> (accessed Jun 2nd, 2022).
- [20] P. Straton, *International Heat Treatment and Surface Engineering* **7(2)** (2013) 70-73.
<https://doi.org/10.1179/1749514813Z.000000000053>
- [21] G. C. Allen, J. M. Dyke, S. J. Harris, A. Morris, *Oxidation of Metals* **29** (1988) 391-408.
<https://doi.org/10.1007/BF00666841>
- [22] L-M. Liu, P. Crawford, P. Hu, *Progress in Surface Science* **84(5-6)** (2009) 155-176.
<https://doi.org/10.1016/j.progsurf.2009.01.002>

